EXPERIMENTAL EVALUATION OF THE LATERAL MIXING OF FUEL IN A FLUIDIZED BED WITH CROSS-FLOW OF SOLIDS – INFLUENCE OF TUBE BANKS

Jens Olsson[1], Joakim Larsson[1], Erik Sette[1],

David Pallarès[1*], Srdjan Sasic[2], Filip Johnsson[1]

[1]Department of Energy and Environment, [2]Department of Applied Mechanics

Chalmers University of Technology, SE-41296 Göteborg, Sweden

**Email: david.pallares@chalmers.se*

Abstract – This work investigates the lateral fuel mixing in fluidized beds with a cross-flow of solids by means of experiments in a fluid-dynamically downscaled unit of the Chalmers indirect biomass gasifier. Fuel lateral mixing is expressed as the combined effect of fuel dispersion and drag from the solids cross flow, and the work evaluates quantitatively these two effects at two different fluidization velocities. In addition, the work investigates the influence of a bank of horizontal tubes. It is found that there is a significant increase in both lateral fuel dispersion and drag of the fuel particles with fluidization velocity. Furthermore, the two mechanisms for lateral fuel mixing are drastically lowered by the insertion of the tube bank.

INTRODUCTION

In a fluidized bed gasifier solid fuel is converted to a product gas through endothermic reactions. In the case of indirect gasification a dual fluidized bed (DFB) system is used in which heat for the endothermic gasification process is supplied by means of solids circulation between the gasifier bed and a combustor, i.e. hot solids enter the gasifier from an external fluidized bed combustor (see e.g. Hofbauer et al. 1997 for details on the process). Inside the gasification reactor, fuel is dried and devolatilized and the remaining char is gasified (typically with steam). Char gasification under fluidized bed conditions, i.e. for large fuel particles and temperatures around 800-900 °C, is typically slow and thus governed by the fuel residence time in the gasifier. The final components in the product gas from indirect gasification consist mainly of volatile matter and char gasification products (hydrogen and carbon monoxide), which represent a product gas with a higher heating value than that obtained through direct gasification. The latter also contains combustion products and nitrogen (if air is used as oxidizer carrier).

In indirect gasifiers the lateral fuel dispersion process is of great importance since it has a strong influence on to what extent the char is gasified within the gasifier bed, thereby having a large impact on the product gas yield and the thermal balance of the process. Whereas high fuel mixing is desired in fluidized bed combustion units, indirect gasifier beds will benefit from limited lateral fuel mixing to ensure a high enough char residence time to maximize the gas yield. Most research with respect to the lateral mixing of fuel in fluidized beds has been carried out without cross-flow of solids, such as the experimental works carried out in large scale units by Niklasson et al. (2002), Chirone et al. (2004) and Liu et al. (2010). Thus, it is not known to what extent cross-flow of solids will influence the lateral fuel mixing in a fluidized bed.

This work studies lateral fuel mixing in a cold fluid dynamically downscaled model of the Chalmers 4MW gasifier (see Thunman and Seemann, 2010 for details on the unit) with a cross-flow of solids for different fluidization velocities. In addition, the effect of a horizontal tube bank is evaluated.

THEORY

Fuel mixing in fluidized beds is induced by both the bubble flow and by cross-flow of solids induced by the circulating bed material as is present in DFB such as applied in indirect gasifiers. The lateral fuel mixing induced by the bubble flow can be seen as dispersive on a macroscopical scale and can therefore be expressed as an isotropic random mixing process (Kunii and Levenspiel, 1991). This was experimentally proven by Olsson et al. (2012) to be the case in the Chalmers gasifier using biomass as fuel. Thus, fuel dispersion caused by the bubble flow can be described by a dispersion coefficient, D_f. The velocity field in the horizontal plane induced by the cross-flow of bulk solids imposes a horizontal drag on the fuel particles and can therefore be expressed as a convective process (and is hereafter referred to as the convective component of the lateral fuel mixing). This work applies a 2 dimensional description of the lateral fuel mixing to determine the horizontal fuel transport in the horizontal plane in the direction from the fuel inlet to the fuel outlet of the bed. The following transport equation is obtained for the fuel phase:

$$\frac{\partial(C)}{\partial t} + \mathrm{div}(C\,\theta\,\boldsymbol{u}) = \mathrm{div}\left(D_f\ \mathrm{grad}\ C\right) \qquad \textbf{(1)}$$

where the transported scalar C denotes the fuel concentration, D_f is the lateral fuel dispersion coefficient and u the velocity field induced by the cross-flow of bulk solids. The cross-flow impact factor, θ, describes how well the fuel phase follows the velocity field of the bulk solids, $\boldsymbol{u}$, with $\theta = 1$ representing no slip between fuel particles and the velocity field induced by the cross-flow while $\theta = 0$ that the solids cross flow has no impact on the motion of the fuel particles. The bulk-solids velocity field is derived from the assumption that the lateral mixing of bulk solids in a bubbling bed consists of a random isotropic process (as discussed above for the fuel solids) which yields a dispersive mixing.

EXPERIMENTAL SETUP

In order to study the fuel mixing in the Chalmers biomass gasifier, a fluid dynamically down-scaled model operating at ambient temperature has been used. A downscaled unit allows not only for increased flexibility in the operation and data sampling, but also facilitates test of different bed geometries. Details of the cold model are given elsewhere (Sette et al., 2012). For this work, the cold flow model has been equipped with a screw-based controllable solids recirculation system resembling the solids circulation in the large-scale DFB system. The scaling relationships derived by Glicksman et al. (1994) from the governing equations for multiphase flow has been applied and the resulting groups which should be kept constant during scaling are listed in Table 1.

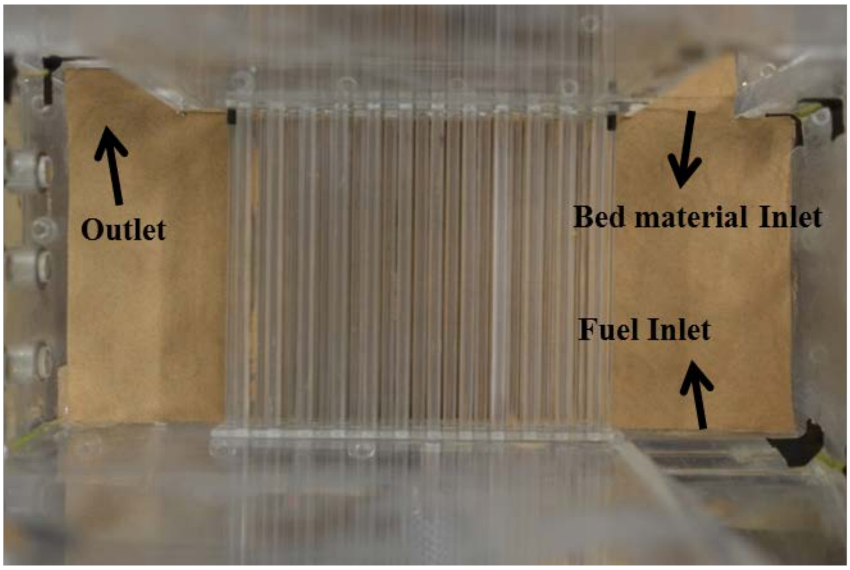

Figure 1: The bed cross-section seen from above with the tube bank inserted.

Table 1: Dimensionless scaling numbers as obtained from Glicksman et al. (1994).

Relation	1	2	3	4	5	6
Group	$\frac{u_0^2}{gL}$	$\frac{\rho_s}{\rho_g}$	$\frac{\rho_s u_0 d_p}{\mu}$	$\frac{\rho_g u_0 L}{\mu}$	$\frac{G_s}{\rho_s u_m}$	Bed geometry

The parameters at hot and cold downscaled conditions can be seen in Table 2. The determination of the parameters for the downscaled tests starts with the use of relation 2: given the gas and solids density at hot conditions and imposing the use of ambient air at cold conditions leads to the use of heavy particles (8900 kg/m^3) at cold conditions. The use of ambient air combined with relations 1 and 4 gives the geometrical scaling factor (1/6). Thereafter, the solids size in the scale model can be determined with relation 3 (yielding 75 µm), the fluidization velocity with relation 1 (see values in Table 2) and the solids recirculation with relation 5 (yielding 0.181 kg/s). In addition, a horizontal "tube" bank (of acrylic glass rods) was installed at the center of the bed as shown in Figure 1, with the tubes perpendicular to the cross-flow of solids and extended over the reactor width covering half of the length of the reactor (in all the tube bank covers 50% of the bed cross-section).

The tube bank is a downscale of a typical tube bank used in fluidized bed heat exchangers, being at large scale 0.36 m-high and with upper tube row at the same level as the fixed bed height. The tubes have a diameter of 30 mm with a triangular pitch of 75 mm. Using Glicksman's scaling relationships, values for the superficial gas velocity, bed height and solids mass flow rate in the cold flow model were calculated which resemble operation in the Chalmers gasifier (Table 2). A higher fluidization velocity was also tested (cases C and D) and each condition was run also with the tube bank (cases B and D).

Table 2: Experimental operating conditions

	Case			
	A	**B**	**C**	**D**
Tube Bundle installed	No	Yes	No	Yes
Chalmers gasifier operating conditions				
Superficial gas velocity, u_0 (m/s)	0.16		0.23	
Bed height (cm)	42			
Solids mass flow rate (kg/s)	4.2			
Solids density (kg/m^3)	2600			
Solids average particle size (µm)	425			
Cold model operating conditions				
Superficial gas velocity, u_0 (m/s)	0.064		0.098	
Bed height (cm)	7			
Solids mass flow rate (kg/s)	0.181			
Solids density (kg/m^3)	8900			
Solids average particle size (µm)	75			

The fuel particles in the gasifier will change in density as they pass the gasifier bed, i.e. during conversion from wet wood to char. Thus, the density is assumed to be the average between a wood pellet (~1175 kg/m^3) and char (233 kg/m^3), i.e. 700 kg/m3. Perfect scaling of such particles would require a density of 2400 kg/m^3 which is very close to aluminum 2700 kg/m^3 which was applied. The wood pellets used in the gasifier have a diameter of 8 mm and an average length of 16 mm, which led to the use of 2-3 mm-long pieces of 1.5 mm o.d. aluminum wire to represent the fuel particles.

In the experimental method, a batch consisting of 1000 down-scaled fuel particles was inserted in the fuel inlet of the scale model and collected at the outlet, with time intervals depending on the superficial gas velocity and bed configuration. The transient curves obtained were matched to Eq. 1 applying the least square method, thus providing the corresponding values of the fuel lateral dispersion coefficient, D_f, and the cross-flow impact factor, θ.

RESULTS

Figure 2 shows the transient curves of outlet fuel concentration as obtained from the experiments together with the corresponding model fits. As can be seen the higher velocity (Cases C and D) yields a more rapid mixing as well as that the fuel mixing is drastically reduced by insertion of the tube bank (Cases B and D). Case A was repeated in order to study the amount of tests needed for statistically robust data; all data points from all tests for case A (thus higher than for the other cases) are included in Fig. 2.a.

Table 3 shows the up scaled values for the lateral fuel dispersion, D_f, and the cross-flow impact factor, θ. Values in Table 3 have experimental error spans of typically 7% for the dispersion coefficient and

6% for the cross-flow impact factor. As seen, both D_f and θ (dispersion and the convection by bulk solids cross-flow) increase with increased fluidization velocity. The cross-flow impact factor also increases with fluidization velocity, meaning that the fuel follows the solids cross flow to a larger extent than at low fluidization velocity.

For the cases without a tube bank, the lateral fuel dispersion coefficient is found to be $2.38 \cdot 10^{-3}$ m^2/s for the lower fluidization velocity (Case A) and $6.17 \cdot 10^{-3}$ m^2/s, for the higher velocity (Case C).

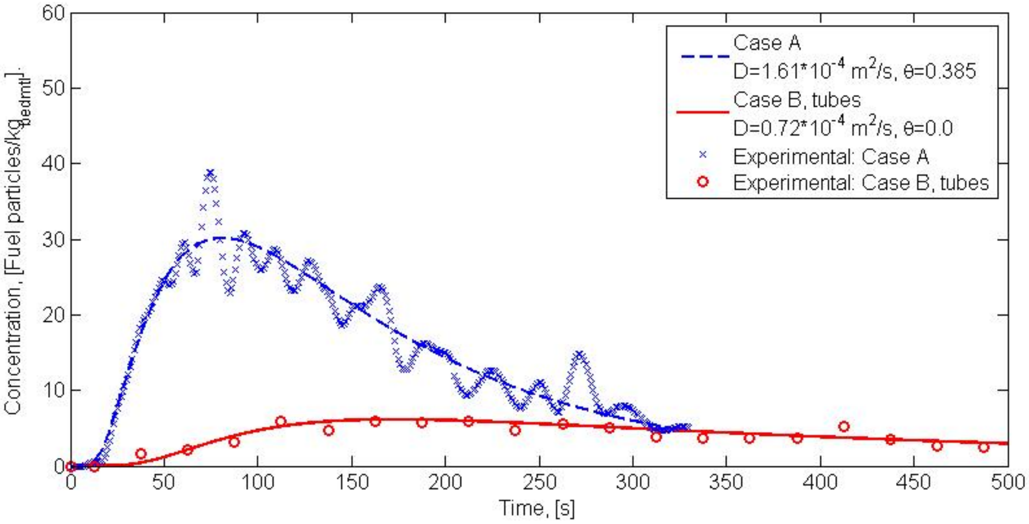

a)

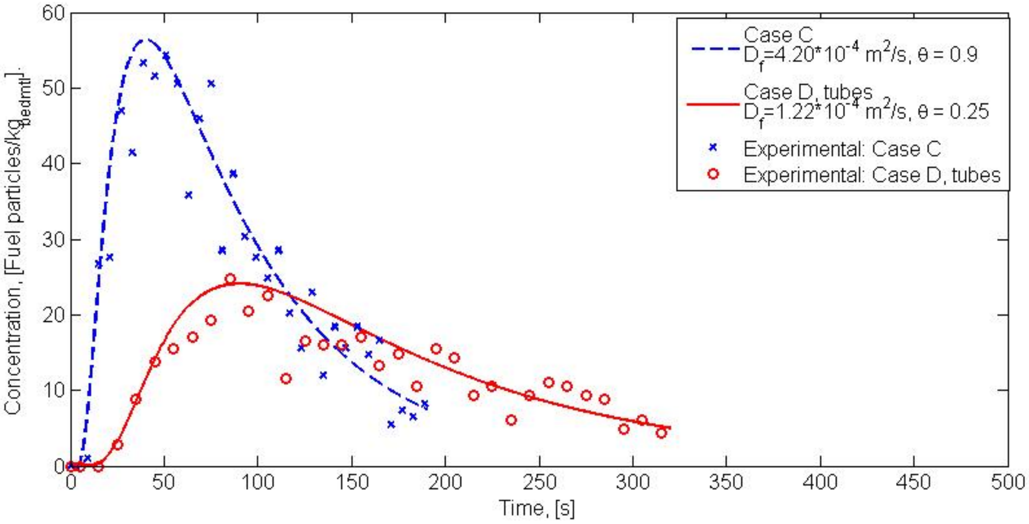

b)

Figure 2: Experimental and modelled transient fuel concentration at reactor outlet as measured (i.e. downscaled values). a) cases A and B b) cases C and D.

Table 3: Experimentally-obtained values of the fuel lateral dispersion coefficient and cross-flow impact factor for the cases studied. Up-scaled values.

	Case			
	A (ref.)	**B**	**C**	**D**
Tube Bundle installed	No	Yes	No	Yes
u_0 - Superficial gas velocity (m/s)	0.16		0.23	
$\boldsymbol{D_f}$ **-** Fuel lateral dispersion coefficient (m^2/s)	$2.38 \cdot 10^{-3}$	$1.07 \cdot 10^{-3\,*}$	$6.17 \cdot 10^{-3}$	$1.79 \cdot 10^{-3\,*}$
$\boldsymbol{\theta}$ **-** Cross-flow impact factor	0.38	0 *	0.90	0.25 *

* These values are applied only to the tube bundle region,
values at freely bubbling conditions are applied elsewhere in the bed

For cases in which the tube bank was inserted, the values of D_f and θ experimentally obtained for the corresponding run without tube bank were applied to the freely bubbling regions of the bed (see Fig. 1). Having this, local values of D_f and θ could be defined in the model for the tube bank region and thus obtained by fitting to the experimental curves obtained. As seen in Table 3, the insertion of tubes yielded values of D_f in the tube bundle region of $1.07 \cdot 10^{-3}$ m^2/s and $1.79 \cdot 10^{-3}$ m^2/s for the lower and higher fluidization velocities tested, respectively. The fuel particles follow the bulk solids cross-flow to a significant extent (θ = 0.38–0.90) in the cases without tubes (with a higher impact factor at the higher fluidization velocity; Case C), but are strongly decoupled from the cross-flow (θ =0 and 0.25, respectively) in the region covered by the tube bank. This shows that tube banks reduce the dispersive mixing (by 70%) as well as the convective mixing (from 40% to 100%) of the fuel particles, thereby increasing the residence time of the fuel.

During the experiments at low fluidization velocity it was found that a significant portions of the fuel particles accumulated at the walls close to the fuel inlet, especially with the tubes inserted (Case B). Thus, the lower lateral mixing observed for the low velocity cases (Cases A and B) can be partially explained from an increased wall effect.

CONCLUSION

The lateral fuel lateral dispersion process in bubbling fluidized beds with a significant cross flow of solids has been investigated in a fluid dynamically down-scaled model of the Chalmers biomass gasifier.

Experimental data on transient fuel concentration at the bed outlet shows that lateral mixing of fuel particles can be described by the sum of two mixing mechanisms: dispersive mixing corresponding to the mixing induced by the bubble flow and convective mixing corresponding to the impact from the solids cross-flow on the fuel particles.

The lateral mixing of fuel is found to increase significantly by increasing the fluidization velocity due to the increase of both the dispersive mixing and the ability of the fuel particles to follow the convective flow originated by the solids cross flow. The two mechanisms for fuel lateral mixing are both drastically lowered by insertion of the tube bank.

NOTATION

C	Concentration, [kg/m^2]
D_{bm}	Lateral dispersion coefficient for bed material, [m^2/s]
D_f	Lateral dispersion coefficient for fuel particles, [m^2/s]
G_s	Solids flux, [kg/m^{2}s]
L	Length, [m]
d_p	Particle diameter, [m]
g	Gravitational constant, [m/s^2]
t	Time, [s]
u_0	Superficial gas velocity, [m/s]
$\boldsymbol{u}$	Velocity field, [m/s]
θ	Cross-flow impact factor, [-]
μ	Dynamic viscosity, [kg s^{-1} m^{-1}]
ρ_g	Density of fluidization medium, [kg/m^3]
ρ_s	Density of solids, [kg/m^3]

REFERENCES

Chirone, R., F. Miccio, Scala, F. 2004. On the relevance of axial and transversal fuel segregation during the FB combustion of a biomass. Energy and Fuels, 18(4), pp.1108-1117.

Glicksman, L.R., Hyre, M.R., Farell, P.A. 1994. Dynamic similarity in fluidization. International Journal of Multiphase Flow, 20, pp.331-386.

Hofbauer, H., Veronik, G., Fleck, T., Rauch, R. 1997. The FICFB gasification process. Developments in Thermochemical Biomass Conversion, vol. 2. Bridgwater and Boocock Eds., pp.1016–1025.

Kunii, D., Levenspiel, O. 1991. Fluidization Engineering. Butterworth-Heinemann Eds.

Liu, D., Chen, X. 2010. Lateral solids dispersion coefficient in large-scale fluidized beds. Combustion

and Flame, 157, pp.2116-2124.
Niklasson, F., Thunman, H., Johansson, F., Leckner, B. 2002. Estimation of solids mixing in a fluidized bed combustor. Industrial & Engineering Chemistry Research, (41)18, pp.4663-4673.
Olsson, J., Pallarès, D., Johnsson, F. 2012. Lateral fuel dispersion in a large-scale bubbling fluidized bed. Chemical Engineering Science, (74), pp.148-159.
Sette, E., Gómez-García, A., Pallarès, D., Johnsson, F., 2012, Quantitative Evaluation of Inert Solids Mixing in a Bubbling Fluidized Bed. Proc. The 21st International Conference on Fluidized Bed Combustion, pp. 573-580.
Thunman, H., Seemann, M. 2010. First experiences with the new Chalmers gasifier. Proc. of the 20th International Conference on Fluidized Bed Combustion, pp.659-663.